Photoelectrochemical Reduction of a Cu(I) Complex to Copper Metal by Hot Electrons at p-InP

Carl A. Koval* and Peter R. Segar

Contribution from the Department of Chemistry and Biochemistry, University of Colorado, Campus Box 215, Boulder, Colorado 80309. *Received August 1, 1988*

Abstract: The chemically irreversible reduction of copper(I)(*trans*-diene)$^+$ to copper metal has been used to confirm the existence of hot-electron processes at the p-InP/acetonitrile interface. Although hot-carrier processes have been previously reported, this is the first observation of a chemical product produced by a hot-carrier reaction in a photoelectrochemical cell. Band-edge positions have been determined by capacitance measurements done under conditions identical with the hot-carrier copper-plating experiments. Supraband-edge production of Cu(0) occurred at high-doped (1.2×10^{18} cm^{-3}) p-InP but was not observed at low-doped (8×10^{15} cm^{-3}) samples. For the high-doped electrode, a quantum yield for production of copper by hot electrons of 0.25% was measured, but this represents only a lower limit to the actual quantum yield for hot electrons since the hot-carrier probe reaction must compete with other processes. Nearly identical quantum yields were measured with both 632.8- and 543.5-nm illumination; however, the intensity profile across the electrode surface has a dramatic effect on the quantum yield.

Hot-carrier charge-transfer processes are important in solid-state systems[1a,b] and have been predicted to occur in photoelectrochemical systems.[2,3] Hot-carrier effects have the potential to enhance conversion efficiencies in photoelectrochemical cells (PEC's).[4] There is experimental evidence that hot-carrier effects result in enhanced photocurrents in III–V semiconductor systems,[5] however, until now, no distinct chemical product produced by hot carriers has been reported. This paper describes hot-electron reductions, which have been observed at the p-InP/acetonitrile interface, resulting in plating of copper metal on the surface of p-InP, a supraband-edge reaction.

When a p-type electrode in depletion is illuminated with photons having energies greater than the band gap of the semiconductor, it is generally thought that the excited electrons are thermalized as they travel through the depletion region, ultimately being ejected into the solution at the energy either the conduction band edge or of surface states within the band gap.[6] Thermalization represents one of the greatest contributions to power loss in PEC's. Hot-carrier processes occur when the thermalization processes are slow with respect to the time required for the photogenerated electron to travel through the depletion region, thus the electron is ejected with a conservation of a greater fraction of the initial photon energy than a completely thermalized electron. Figure 1 illustrates two different possible hot-carrier processes, which have been discussed by Nozik et al.[5] In type I processes, electrons are fully thermalized to the bottom of the conduction band while still in the bulk are not completely thermalized to the energy of the band edge as they travel through the space charge region. Type II hot carriers are never fully thermalized and are ejected into the solution with energies greater than the conduction band in the bulk. In the solid state, hot-carrier processes can be quite efficient,[7] but the interface between a semiconductor and a solution may represent a formidable barrier to electron transfer in PEC's.

Hot carriers are most likely to occur in semiconductors having high charge carrier mobilities, low minority carrier effective masses, and high-doping densities.[2,8] For this reason, III–V semiconductors such as InP, which have relatively high electron mobilities, are expected to be excellent for observation of hot-carrier phenomena (see Table I for a summary of important physical constants for InP). Under conditions of high band bending, the depletion region is relatively narrow, and the electric field present at the surface is very high. It has also been shown that a thin depletion region along with low effective minority carrier mass leads to greater quantization in the depletion region, thus a longer time constant for thermalization.[2]

Table I. InP Constants

band gap at 300 K	E_{bg}	1.35 eV
electron mobility	μ_{e^-}	4600 cm^2/V·s
electron effective mass	m^*	0.077
static dielectric	ϵ	12.4

Solid-state measurements such as picosecond luminescence[9a] and Raman spectroscopy[9b] have shown that hot-carrier mechanisms can be very important; they even form the basis of the operation of important devices such as the negative electron affinity photocathode[10a] and the hot-electron transistor.[10b] Observing hot carriers in photoelectrochemical systems has been much more difficult because there is no simple way to determine the energy of electrons as they are ejected into a solution.

Experimental evidence for hot electrons at p-GaP[11] and p-InP[5,12] in photoelectrochemical systems has been provided by Nozik et al. In their experiments, significant photocurrents were observed in the presence of redox species having reversible reduction potentials negative of the conduction band edge. Other reports of apparent supraband-edge reactions have been complicated by band-edge movement.[13a,b]

We have used an irreversible chemical reaction to trap hot electrons produced at the p-InP/acetonitrile interface. Copper(II) 5,7,7,12,14,14-hexamethyl-1,4,8,11-tetraazacyclotetradeca-4,11-diene, copper(II)(*trans*-diene)$^{2+}$, can be reversibly reduced by one electron to form copper(I)(*trans*-diene)$^+$ (see Figure 2 for structure). The Cu(I) complex can further be reduced by one more electron at potentials significantly negative of the InP conduction band edge. This irreversible reaction results in plating

(1) (a) Proceedings of the International Conference on Hot Electrons in Semiconductors. *Solid State Electron*, **1978**, 21. (b) Sze, S. M. *Physics of Semiconductor Devices*; Wiley-Interscience: New York, 1981.
(2) Boudreaux, D. S.; Williams, F.; Nozik, A. J. *J. Appl. Phys.* **1980**, *51*(4), 2158.
(3) Nozik, A. J.; Boudreaux, D. S.; Chance, R. R.; Williams, F. *Adv. Chem. Ser.* **1980**, *184*, 162.
(4) Ross, R. T.; Nozik, A. J. *J. Appl. Phys.* **1982**, *53*, 3813.
(5) Cooper, G.; Turner, J. A.; Parkinson, B. A.; Nozik, A. J. *J. Appl. Phys.* **1983**, *54*(11), 6463.
(6) Gerischer, H. *Physical Chemistry: An Advanced Treatise*; Eyring, H., Ed.; Academic: New York, 1970; Vol. 9, pp 463–542.
(7) Keyes, R. W.; Nathan, M. I. *IBM J. Res. Dev.* **1981**, *25*(5), 779.
(8) Buhks, E.; Williams, F. In *Photoelectrochemistry: Fundamental Properties and Measurement Techniques, Electrochemical Society Symposium Proceedings*; Wallace, W., Nozik, A. J., Deb, S. K., Wilson, R., Ed.; Electrochemical Society: New Jersey, 1981.
(9) (a) Kash, K.; Shah, I.; Block, D.; Gossand, A. C.; Wiegmann, W. *Physica* **1985**, *134B*, 189. (b) Tsang, J. C.; Kash, J. A.; Jha, S. S. *Physica* **1985**, *134B*, 184.
(10) (a) Willardson, R. K.; Beer, A. C. *Semiconductors and Semimetals*; Academic: New York, 1981; Vol. 15, pp 195–300. (b) Sze, S. M. *Physics of Semiconductor Devices*; Wiley-Interscience: New York, 1981; p 184.
(11) Turner, J. A.; Nozik, A. J. *Appl. Phys. Lett.* **1982**, *41*(1), 101.
(12) Turner, J. A.; Thacker, B.; Nozik, A. J. *Hot Carrier Effects at the Semiconductor Electrolyte Interface*. Proceedings of Electrodynamics and Quantum Phenomena at Interfaces, Telavi, Georgia, USSR, 1984.
(13) (a) Turner, J. A.; Manassen, J.; Nozik, A. J. *Appl. Phys. Lett.* **1980**, *37*(5), 488. (b) Kohl, P. A.; Bard, A. J. *J. Electrochem. Soc.* **1979**, *126*(4), 598.

0002-7863/89/1511-2004$01.50/0

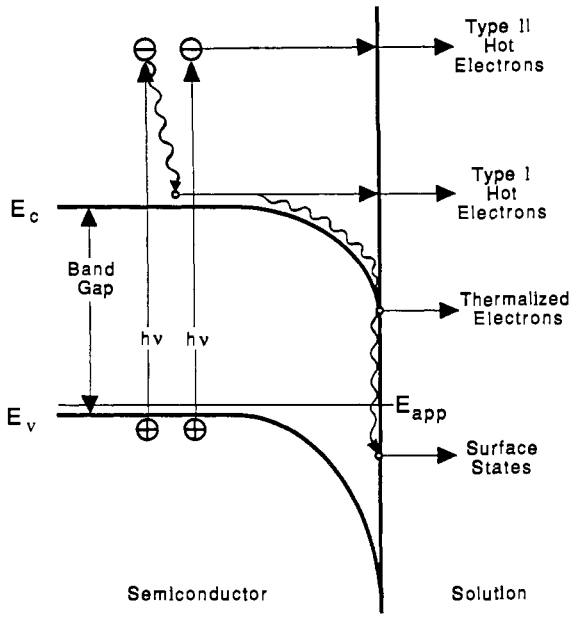

Figure 1. Fates of photogenerated electrons in a p-type electrode in depletion.

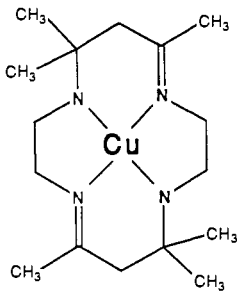

Figure 2. Structure of copper(II) 5,7,7,12,14,14-hexamethyl-1,4,8,11-tetraazacyclotetradeca-4,11-diene, or copper(II)(*trans*-diene)$^{2+}$.

of copper metal on the surface of the electrode.[14] Anodically stripping this film is a highly sensitive means of determining the exact amount of Cu(0) product produced via reaction with hot electrons. Unambiguous observation of hot carriers depends upon being able to determine the potential of the band edges; this was accomplished by using capacitance measurements under the exact conditions of the plating experiment. Reductions at dark n-InP electrodes in the accumulation condition were used to determine the potential at which reduction of copper(I)(*trans*-diene)$^+$ begins to occur at metal-like InP electrodes.

All results herein are discussed within the framework of the Gerischer[6] model of the semiconductor/electrolyte interface. The application of classical equations is intended to aid in describing trends in the experimental data rather than to suggest a theoretical basis for understanding the supraband-edge reactions that have been observed. Advanced quantum mechanical models have been developed that rigorously describe hot-carrier processes in the solid state.[15,16]

Experimental Section

Reagents and Materials. UV-grade acetonitrile (Burdick-Jackson) was doubly distilled under nitrogen first over P_2O_5 and then over CaH_2. Tetrabutylammonium fluoroborate, TBAFB (Southwestern Analytical) was recrystallized twice from absolute ethanol, and dried under vacuum for 3–5 days. [Copper(II)(*trans*-diene)]$(ClO_4)_2$ was prepared according to the procedure outlined by Olson and Vasilevskis[17] and modified by Allison.[18] All solutions were 0.1 M in TBAFB and had a total copper complex concentration of 5.0 mM. Solutions were electrolyzed prior to the experiment to yield a poised solution containing a 95:5 ratio of copper(II)(*trans*-diene)$^{2+}$/copper(I)(*trans*-diene)$^+$. The rest potentials of these solutions were −0.87 V vs ferrocene.[19]

Photochemical Measurements. All measurements were performed in a Vacuum Atmospheres helium-filled glovebox. The three-electrode electrochemical cell and basic electrochemical equipment have been described previously.[20] The $Ag/AgNO_3$ reference electrode had a potential of +0.100 V vs ferrocene. All potentials are reported vs the $Ag/AgNO_3$ electrode unless otherwise noted. The Mott–Schottky data acquisition was performed as previously described[20] with the exception of the computer used to control the experiment. An IBM PC with a Data Translations 2801-A Analog and Digital I/O Board was used with acquisition software written by Dr. John Turner of the Solar Energy Research Institute.

For illuminated experiments, either a Melles-Griot 5-mW red HeNe laser (632.8 nm, 1.96 eV) or a Melles-Griot 0.5-mW green HeNe (GreNe) laser (543.5 nm, 2.28 eV) was used. The beams were defocused to an area approximately 10 times greater than the electrode area for most experiments; however, for some experiments the laser was defocused to an area smaller than the electrode. With the beam defocused to a large area, the intensity across the electrode surface was uniform to within 5%, while with the smaller beam area, the intensity varied by over 100% from the center to the edge of the electrode. For this reason, we will refer to these as "uniform illumination profile" and "variable illumination profile" experiments, respectively. Actual intensity profiles are presented in the Discussion.

Light intensities were adjusted with neutral-density filters and were measured with an Oriel 7072 photodiode readout equipped with a 7052 UV–vis vacuum photodiode detector and a diffuser. Accurate light intensities and photon flux measurements were crucial, so all values have been corrected for reflection loss and solution absorption losses.

The reflection loss occurring at a solid with a refractive index n_1 immersed in a solution of refractive index n_2 is given by[21]

$$R = \frac{(n_1 - n_2)^2 + n_1^2}{(n_1 + n_2)^2 + n_1^2}$$

where n_1 is the imaginary refractive index of the solid phase, which is given by $n_1 = \alpha c/2\omega$, where α is the absorption coefficient of the solid phase, 10 and 5 μm^{-1} for InP at 543.5 and 632.8 nm, respectively.[22] Thus, the amount of light lost by reflection was 21 and 18%. The solution absorption loss corrections were done by spectrophotometrically measuring the absorbance of the solutions following each experiment.

Electrode Preparation and Pretreatment. Bent InP electrodes were constructed as previously described.[20] Single-crystal InP wafers were obtained from Crysta-Comm, and had (100) crystal orientation. p-type electrodes were Zn doped at 8×10^{15} (low-doped samples) and 1.23×10^{18} cm^{-3} (high-doped samples) as reported by the manufacturer; n-type electrodes were tin doped to 1.22×10^{18} cm^{-3}.

All InP electrodes were prepared before each experiment by a slightly modified bromine etching procedure originally reported by Aspnes.[23] Electrodes were etched for 30 s in 5% Br_2/MeOH and then chemomechanically polished with lens paper and 0.05% Br_2/MeOH. They were then etched for 20 s in 5% Br_2/MeOH, rinsed with water, and then subjected to 50% NH_4OH in water for 30 s to remove remaining bromides. Finally, the electrodes were rinsed thoroughly with water, dried with N_2, and immediately transferred to the antechamber of the glovebox. The resulting InP surfaces were mirror smooth, reproducible, and electrochemically well-behaved.[24]

Hot-Carrier Experimental Procedure. Hot-carrier experiments were performed on both high- and low-doped p-InP electrodes under different amounts of band bending and with light of two different wavelengths. Experiments were reproduced on different days using different electrodes. In all cases, p-type electrodes in the 5 mM copper complex solution exhibited negligible dark currents when biased at potentials within the depletion region.

(14) Kolthoff, I. M.; Coetze, J. F. *J. Am. Chem. Soc.* **1957**, *79*, 1852.
(15) Niez, J. J.; Ferry, D. K. *Phys. Rev. B* **1983**, *28*(2), 889.
(16) Zimmerman, J.; Luigi, P.; Ferry, D. K. *J. Phys. Colloq.* **1981**, *42 C-7*, 95.
(17) Olson, D. C.; Vasilevskis, V. *Inorg. Chem.* **1971**, *10*(3), 463.
(18) Allison, J. C. Ph.D. Thesis, California Institute of Technology, 1979.
(19) Gagne, R. R.; Koval, C. A.; Lisensky, G. C. *Inorg. Chem.* **1980**, *19*, 2854.
(20) Koval, C. A.; Austermann, R. L.; Turner, J. A.; Parkinson, B. A. *J. Electrochem. Soc.* **1985**, *132*(3), 613.
(21) Hecht, E.; Znjac, A. *Optics*; Addison-Wesley: Reading, MA, 1976; pp 85–89.
(22) Escher, J. S. In *Semiconductors and Semimetals*; Academic Press: New York, 1981; Vol. 15, p 208.
(23) Aspnes, D. E.; Stunda, A. A. *Appl. Phys. Lett.* **1981**, *39*(4), 316.
(24) Segar, P. R.; Koval, C. A. *J. Electrochem. Soc.* **1988**, *135*(10), 2655.

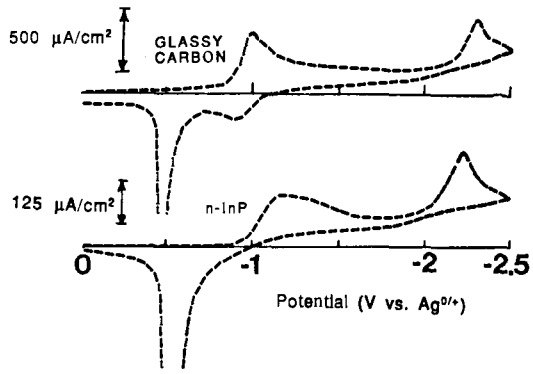

Figure 3. Cyclic voltammograms of 5 mM copper(II)(*trans*-diene)$^{2+}$ at glassy carbon and n-InP in the dark. Scan rate was 200 mV/s.

Before each experiment, Mott–Schottky scans were recorded both in the dark and in the light under the exact conditions of stirring rate, light intensity, and potential range that were to be used in the copper-plating experiments. The electrodes were then illuminated for 30 s while potentiostatically controlling the electrode potential and maintaining a mass transfer rate significantly above the light-limited current with a magnetic stirrer. After the 30-s deposition step, the light was turned off, the solution was stirred further to remove any remaining photogenerated copper(I)(*trans*-diene)$^{+}$ and free ligand, and stirring was turned off. The InP electrode was then scanned anodically in the dark from −1.0 to ca. −0.10 V at 200 mV/s. Manual integration of the anodic stripping voltammogram revealed the total moles of copper metal formed by hot-carrier reactions. After the plating and stripping steps, another Mott–Schottky scan was performed, again under the exact conditions of the experiment.

Identical experiments were performed on n-InP electrodes in the dark. At applied potentials negative of −1.0 V, n-type electrodes entered the accumulation condition and behaved as metal-like electrodes. This allowed us to measure current densities at various potentials for a metal-like InP electrode for comparison with the p-InP electrodes.

Current Density Calculations. Current densities, as opposed to total amounts of charge, have been calculated in order to allow direct comparison of rates for reduction reactions occurring at n-type electrodes with those occurring at p-type electrodes. The reductions were carried out with constant illumination intensity and stirring rate; therefore, charge = current × time. The total current density (J_{total}) was calculated by dividing the total charge passed during an electrolysis by the electrolysis time and the electrode surface area and includes contributions from both copper(II)(*trans*-diene)$^{2+}$ + e$^-$ → copper(I)(*trans*-diene)$^{+}$ and copper(I)(*trans*-diene)$^{+}$ + e$^-$ → Cu(0) + *trans*-diene. Electrode surface areas have been determined by a photographic technique. The stripping current density (J_{strip}) was calculated by manually integrating the anodic stripping wave to obtain the charge passed in stripping the copper film off the electrode and then dividing by the electrolysis time and the electrode surface area.

Results

Copper(*trans*-diene) Electrochemistry and Photostability. Understanding the electrochemistry of the copper complex system is essential for the proper interpretation of the plating experiment results. Cyclic voltammograms of 5 mM copper(II)(*trans*-diene)$^{2+}$ at both glassy carbon and dark n-InP microelectrodes are shown in Figure 3. The reversible wave occurring at −0.97 V corresponds to the reversible one-electron reduction to copper(I)(*trans*-diene)$^{+}$:

$$\text{copper(II)(}trans\text{-diene)}^{2+} + e^- \rightleftharpoons \text{copper(I)(}trans\text{-diene)}^{+} \quad (1)$$

This wave occurs slightly positive of the conduction band edge of p-InP in the plating experiments, so the copper(II)(*trans*-diene)$^{2+}$ species will accept most of the thermalized electrons that reach the surface. This is important because any buildup of excess charge on the surface would result in a shift in the band edges.[24] At n-InP the reversibility of this wave is found to be switching potential dependent, which is consistent with previous work using reversible couples at n-InP.[25] The irreversible reduction wave with peak potentials of −2.3 V at GC and −2.2 V at n-InP is

(25) Koval, C. A.; Austermann, R. L. *J. Electrochem. Soc.* **1985**, *132*(11), 2656.

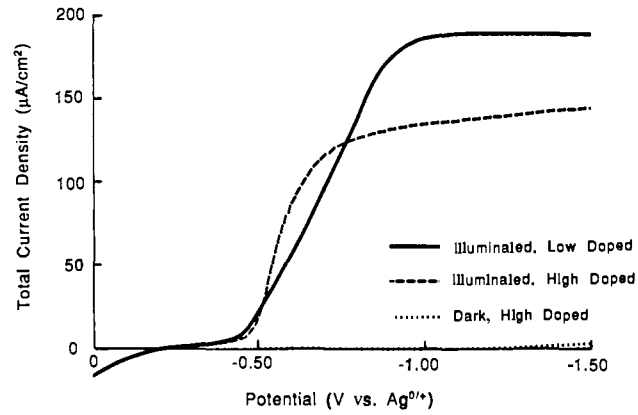

Figure 4. Stirred solution current–voltage curves for p-InP electrodes in 5 mM 95:5 copper(II)(*trans*-diene)$^{2+}$/copper(I)(*trans*-diene)$^{+}$ under 0.594 mW/cm^2 illumination at 543.5 nm.

reduction of copper(I)(*trans*-diene)$^{+}$ to copper metal plus free ligand:

$$\text{copper(I)(}trans\text{-diene)}^{+} + e^- \rightarrow \text{Cu(0)} + trans\text{-diene} \quad (2)$$

The anodic wave at ca. −0.5 V is the one-electron stripping wave for the Cu metal film:

$$\text{Cu(0)} + 4CH_3CN \rightarrow Cu^{I}(CH_3CN)_4^{+} + e^- \quad (3)$$

This wave has a peak potential of −0.35 V on p-InP. $Cu^{I}(CH_3CN)_4^{+}$ can be oxidized to $Cu^{II}(CH_3CN)_4^{2+}$ in CH_3CN at ca. +1.0 V, which is significantly positive of the stripping wave.[14]

Although the second reduction step is chemically irreversible, we have determined the formal reduction potential by measuring the rest potential of a Cu electrode in solutions containing various ratios of [copper(I)(*trans*-diene)$^{+}$]/[*trans*-diene] as produced by bulk electrolysis. A plot of log {[copper(I)(*trans*-diene)$^{+}$]/[*trans*-diene]} vs E_{rest} had a slope of 0.041 and an intercept of $E^{0'}_f$ = −1.37 ± 0.05 V vs Ag(0/1+). The voltammetry experiment reveals that there is a significant overpotential for this reduction at both GC and n-InP.

Photostability of the copper complex solutions under the wavelengths employed is also important even though neither form of the copper complex absorbs at either 632.8 or 543.5 nm. In order to determine a lower limit to the photostability, we illuminated 5 mM 95:5 copper(II)(*trans*-diene)$^{2+}$/copper(I)(*trans*-diene)$^{+}$ solutions with intensities ca. 10 times greater than those used in the plating experiments while monitoring the solution rest potential. The rest potential varied less than 10 mV over a period of a full day, indicating that solutions are stable much longer than the time scale of the plating experiments.

Current–Voltage Curves. Figure 4 shows current–voltage curves for both high- and low-doped p-InP electrodes under 0.594 mW/cm^2, 543.5-nm illumination, as well as a dark current curve for the high-doped sample. These were done under the same conditions of stirring rate and light intensity as the Cu-plating experiments. Very little dark current was observed, so dark current processes can be assumed to be negligible. The current is mainly due to the copper(II)(*trans*-diene)$^{2+}$ + e$^-$ → copper(I)(*trans*-diene)$^{+}$ reduction. Both curves reach a light-limited current density. The diffusion-limited current density was measured at an n-InP electrode in the dark at negative potentials where the electrode is in the accumulation condition. The diffusion-limited current density (J_{dl}) is ca. 700 μA/cm^2, which is several times larger than the light-limited values of 135 and 190 μA/cm^2 for high- and low-doped p-InP samples, respectively. This demonstrates that small fluctuations in stirring rate during the experiments should have no effect on measured current densities.

The low-doped sample exhibited a higher light-limited current density because the space charge region (SCR) was much wider, and a greater portion of the incident light was absorbed there (see Table III). Assuming an optical absorption coefficient, α, for InP of 10 μm^{-1} at 543.5 nm,[22] the electrode is expected to absorb [1 − exp(−αW_d)] × 100% of the incident light in the SCR. When

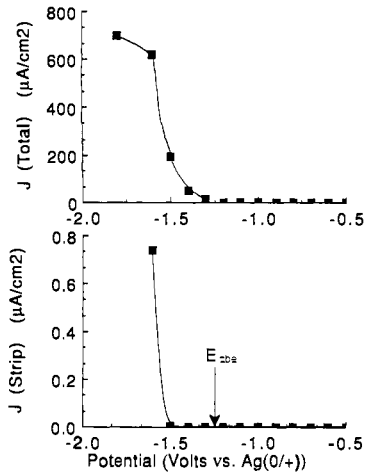

Figure 5. Total (top) and stripping (bottom) current densities for n-InP in the dark in 5 mM 95:5 copper(II)(*trans*-diene)$^{2+}$/copper(I)(*trans*-diene)$^{+}$.

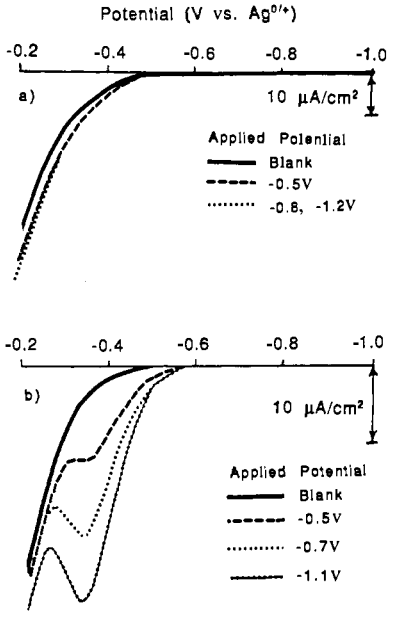

Figure 6. Anodic stripping voltammograms for (a) low-doped p-InP and (b) high-doped p-InP, after 30-s illumination with 0.515 mW/cm^2, 543.5-nm light at various applied potentials in 5 mM 95:5 copper(II)-(*trans*-diene)$^{2+}$/copper(I)(*trans*-diene)$^{+}$.

calculated values of the depletion region width, W_d, at a band bending of 1.0 V (see Table III), are used, the low-doped sample should absorb ca. 95% of the incident light in the SCR and the high-doped sample ca. 26%. Comparing the photocurrent with the incident photon flux reveals that 75% of the photogenerated minority carriers were collected by the low-doped electrodes, while 54% were collected by the high-doped electrodes. The diffusion length for InP is roughly 2 μm,[26,27] which is considerably larger than either W_d (300 Å) or $1/\alpha$ (1000 Å). Thus, for the high-doped sample, light that is absorbed in the bulk still contributes to the photocurrent. This explains the seemingly high collection efficiency for the high-doped electrodes.

Reductions at Dark n-InP. A crucial part of these experiments is determining the potentials at which we begin to observe plating of copper metal under the conditions of the p-type plating experiments. Mott–Schottky experiments reveal that the conduction band edge of this n-InP electrode was at −1.25 V and that the electrode began to enter the metal-like accumulation condition at ca. −1.1 V, so at potentials negative of −1.1 V the n-InP electrode behaves as a metal-like InP electrode.

Figure 5 shows total and stripping current densities (J_{total} and J_{strip}) for a plating experiment performed on an n-InP electrode. The relative magnitudes of the total and stripping currents reveal that, at −1.6 V, less than 1/1000 of the current observed is due to plating of copper. This is consistent with the cyclic voltammograms, which indicated a significant overpotential for copper deposition. It should be noted that there is absolutely no formation of copper metal at potentials positive of −1.5 V.

Uniform-Illumination Profile Photoelectrolysis at p-InP. The p-type hot-carrier experiments were performed on both low- and high-doped electrodes at both 632.8 and 543.5 nm with the laser defocused to yield a uniform illumination profile across the electrode surface. Figure 6a shows the anodic stripping voltam-

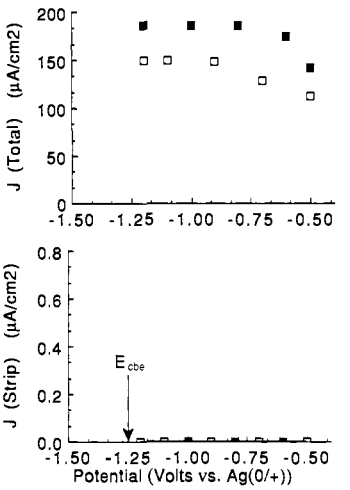

Figure 7. Total (top) and stripping (bottom) current densities for low-doped p-InP. No copper deposition is observed. Open squares are 0.515 mW/cm^2, 632.8 nm; closed squares are 0.594 mW/cm^2, 543.5 nm.

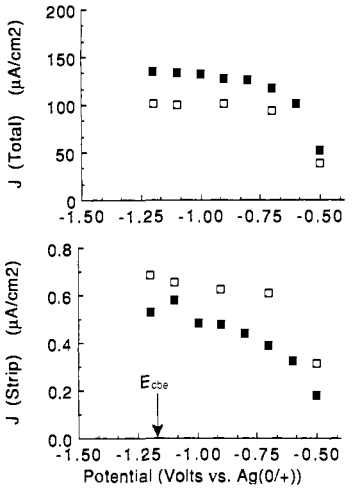

Figure 8. Total (top) and stripping (bottom) current densities for high-doped p-InP. Open squares are 0.515 mW/cm^2, 632.8 nm; closed squares are 0.594 mW/cm^2, 543.5 nm.

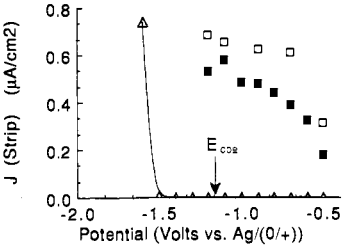

Figure 9. Comparison of stripping current densities at n-InP in dark (open triangles) with illuminated high-doped p-InP (squares). Open squares are 0.515 mW/cm^2, 632.8 nm; closed squares are 0.594 mW/cm^2, 543.5 nm.

(26) Lewis, N. S. *J. Electrochem. Soc.* **1984**, *131*(11), 2496.
(27) Heller, A.; Miller, B.; Lewerenz, H. J.; Bachmann, K. J. *J. Am. Chem. Soc.* **1980**, *102*, 6556.

Table II. Experimental Parameters for All Experiments

	uniform-intensity profile				variable-intensity profile			
	543.5 nm		632.8 nm		543.5 nm		632.8 nm	
	high	low	high	low	high	low	high	low
intensity,[a] mW/cm^2	0.515	0.515	0.594	0.594	0.796	0.796	0.884	0.884
area,[b] cm^2	0.195	0.160	0.195	0.233	0.0707	0.0707	0.0707	0.0707
doping density,[c] cm^{-3}	1.60×10^{18}	1.20×10^{16}	1.61×10^{18}	1.56×10^{16}	1.26×10^{18}	1.20×10^{16}	1.51×10^{18}	1.40×10^{16}
flat band potential,[c] V	+0.110	-0.100	+0.085	-0.037	+0.004	-0.230	-0.040	-0.080
conduction band,[c] V	-1.19	-1.27	-1.22	-1.21	-1.29	-1.40	-1.34	-1.25
doping density,[d] cm^{-3}	1.56×10^{18}	1.25×10^{16}	1.61×10^{18}	1.25×10^{16}	1.23×10^{18}		1.49×10^{18}	1.40×10^{16}
flat band potential, V[d]	+0.080	-0.070	+0.092	-0.032	-0.020		-0.050	-0.030
conduction band,[d] V	-1.22	-1.24	-1.21	-1.20	-1.32		-1.35	-1.20
J_{calc}(max),[e] μA/cm^2	250	250	273	273	354	354	382	382
J_{total}(max),[f] μA/cm^2	135	186	102	150	165	233	152	224
J_{strip}(max), μA/cm^2	0.60	0	0.69	0	0.09	0	0.12	0
ϕ_{Cu}(max), %	0.24	0	0.25	0	0.026	0	0.031	0

[a] Light intensity is corrected for reflection and solution losses. [b] Area is the smaller of the electrode area and the illuminated area. [c] Illuminated scans before the copper-plating experiment. [d] Illuminated scans after the copper-plating experiment. [e] Maximum possible current density calculated from the photon flux. [f] Measured light-limited current density. [g] See discussion for explanation.

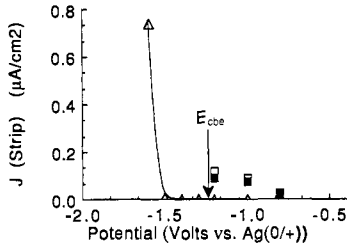

Figure 10. Stripping current densities for variable-intensity profile laser experiment (laser area smaller than the electrode area) using high-doped p-InP. Open triangles are n-InP. Open squares are 0.88 mW/cm^2, 632.8 nm; closed squares are 0.80 mW/cm^2, 543.5 nm.

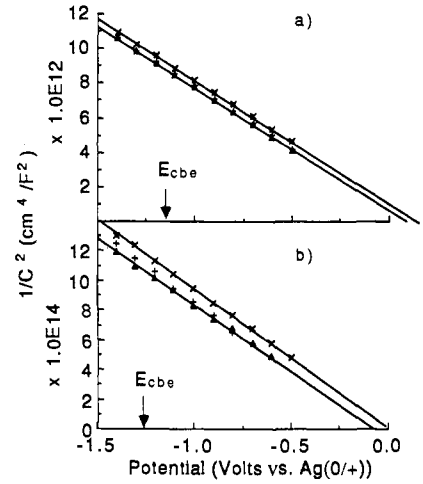

Figure 11. Mott–Schottky plots for (a) high-doped p-InP and (b) low-doped p-InP. ×'s denote a dark scan and +'s are an illuminated scan before the plating experiment; filled triangles are illuminated scans after the plating experiment.

mograms for low-doped p-InP. No stripping is observed at any potential within the depletion region of p-InP. The same is true when 632.8-nm light is used. Figure 7 shows the total and stripping current densities for low-doped electrodes.

Figures 6b and 8 shows that the high-doped electrodes exhibited a significant deposition of copper even though the conduction band edge was at −1.2 V, which is 300 mV positive of the potential at which copper deposition began on n-InP. Again, results at 632.8 nm were similar to those at 543.5 nm. Figure 9 shows the stripping current densities for the high-doped p-type experiment on the same scale as the n-type experiment for comparison. The stripping current densities for high-doped p-InP electrodes under large amounts of band bending were approximately equal to those of the n-InP electrode biased at −1.6 V. Table II contains the important experimental parameters for all p-type experiments.

The surface coverage of copper metal ranged from 0 to 10^{-10} mol/cm^2, which corresponds to 0–4% assuming fcc packing. This copper film can be visually observed and appears to be very smooth and distinctly copper colored. In no case was there any deposition of copper on the sides of the cell or on any nonilluminated p-InP electrode.

Variable-Illumination Profile Reductions. With the laser slightly defocused to an area smaller than the surface of the p-InP electrode, a variable-intensity profile across the electrode is achieved. These experiments were done in the same fashion as the uniform profile experiments, except that the deposition step was 60 s rather than 30 s. The results are summarized in Figure 10 and Table II; the hot-carrier efficiencies were much lower with respect to the uniform-illumination profile experiments. After the deposition step, a small copper spot was observed at the center of the illuminated region of the electrode.

Capacitance Measurements. Accurate determination of the band edges is extremely important for the unambiguous observation of hot carriers. We believe that capacitance measurements are ideally suited for this because they can be performed under the exact conditions of the plating experiment. Other methods such as photocurrent onset and photopotential measurements are less accurate and require higher light intensities. We used low light intensities for these experiments to avoid complication from band-edge movement.

The band-edge positions are derived from capacitance measurements by the following relations[28]

$$\frac{1}{C_{sc}^2} = \frac{2}{\epsilon\epsilon_0 e N_d}\left[E - E_{fb} - \frac{kT}{e}\right]$$

$$E_{vbe} = E_{fb} - kT \ln\left[\frac{N_d}{N_v}\right]$$

$$E_{cbe} = E_{vbe} - E_{bg}$$

where C_{sc} is the capacitance of the space charge region, E_v and E_c are the energies of the valence and conduction band edges, N_d is the doping density, and N_v is the effective density of states in the valence band assumed to be 10^{19} cm^{-3}; all other symbols have their usual meaning.

In all experiments reported in this paper, Mott–Schottky (M–S) plots both before and after plating experiments were nonhysteretic, frequency independent, and reproducible. Doping densities measured by M–S slopes agreed with those provided by the manufacturer to within 25% for the high-doped samples and 50% for the low-doped samples, which is further evidence for the validity of the band edges measured by this method. Figure 11 shows typical M–S plots for both high- and low-doped p-InP electrodes in the dark, under illumination before the plating ex-

(28) Turner, J. A. *J. Chem. Educ.* **1983**, *60*(4), 327.

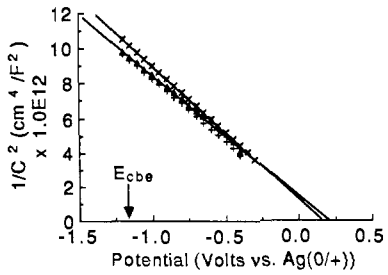

Figure 12. Mott–Schottky plot for a copper-covered p-InP electrode. ×'s are a clean electrode in the dark, +'s are an illuminated clean electrode, and filled triangles are a copper-plated electrode under illumination.

periment, and under illumination after the experiment. Flat band potentials are shifted slightly negative under illumination. M–S results for illuminated p-type electrodes are also summarized in Table II.

It is essential that the M–S plots exhibit no frequency dispersion as it is well-known that frequency dependence is indicative of nonideal behavior[1b,6] and results in unreliable measurements of flat band potentials. The frequency dependence at 500, 5000, and 10000 Hz was measured under conditions identical with the copper-plating experiments. The flat band potentials for the high-doped electrodes were +0.112, +0.110, and +0.111 V respectively, and the doping densities varied by only 3%. The low-doped electrodes exhibited similar frequency independence.

The band edges were stable and reproducible. High-doped electrodes exhibited conduction band edges of −1.20 ± 0.03 V, and low-doped electrodes were −1.25 ± 0.04 V under illumination. Reported uncertainties reflect the standard deviation of eight and six measurements, respectively. Measurements were done on four different p-type electrodes on two different days. The n-type electrode had a conduction band edge of −1.25 V.

M–S plots were also done on a copper-plated p-InP electrode to ensure that a small surface coverage of copper metal (<5%) does not shift the band edges negative. Figure 12 shows M–S plots for an electrode before deposition of the Cu film and after the film has been deposited but not stripped off. The result is that a small amount of copper does not significantly alter the interfacial energetics of the system, which implies that interface states introduced by a low surface coverage of copper metal do not charge enough to shift the band edges under the experimental conditions employed. If the photoelectrolyses are allowed to continue until high coverages (>50% of a monolayer) are obtained, significant band-edge movement is observed.

Discussion

Evidence for Hot-Carrier Processes. Capacitance measurements revealed a very stable and reproducible picture of the energetics of the p-InP/acetonitrile interface. As expected, the conduction band-edge positions for n-type and p-type electrodes were the same to within 50 mV. The band edges did not shift during the plating experiments and were not affected by low surface coverage of copper metal. An interesting finding was that while the M–S slopes remained constant, the flat band potentials shifted slightly negative upon illuminating p-type electrodes. Previous work has shown that the flat band potentials of InP electrodes are dependent upon the solution redox potential.[24] In the dark, no reduction takes place, and the surface of the electrode is exposed to 95:5 copper(II)(*trans*-diene)$^{2+}$/copper(I)(*trans*-diene)$^{+}$. Under illumination significant reduction occurs, causing this ratio to decrease and the redox potential of the solution near the electrode surface to become more negative, thus the flat band potential is shifted slightly negative.

The formal reduction potential for reduction of copper(I)(*trans*-diene)$^{+}$ to copper metal is −1.47 V, which is 0.12–0.17 V negative of the conduction band edge of p-InP. Furthermore, plating experiments and cyclic voltammograms at dark n-InP electrodes have revealed that there is a significant overpotential for reduction of copper(I)(*trans*-diene)$^{+}$ to copper metal and that absolutely no copper metal can be produced at potentials positive of −1.50 V on metal-like InP electrodes under the deposition conditions that were employed. Since the conduction band edges for p-InP are 0.30–0.33 V positive of this, copper deposition must be a supraband-edge reduction. The fact that a significant amount of copper is observed at high-doped p-InP electrodes is direct evidence for hot-electron reduction in a photoelectrochemical cell. The absence of any copper at low-doped p-InP is furthur evidence for hot carriers. If thermalized electrons could reduce copper(I)(*trans*-diene)$^{+}$ at p-InP, we would observe copper at both low- and high-doped electrodes. Also, hot-carrier mechanisms are not expected to be efficient at low-doped electrodes because the depletion region is much wider than similarly biased high-doped electrodes (vide infra).

Quantum Efficiencies. The total current observed in all experiments was the sum of both thermalized and hot photocurrents, copper(II)(*trans*-diene)$^{2+}$ + e$^-$ → copper(I)(*trans*-diene)$^{+}$ and copper(I)(*trans*-diene)$^{+}$ + e$^-$ → Cu(0) + *trans*-diene. At negative potentials, the first reduction took place near the diffusion-limited rate at n-InP and at the light-limited value for p-InP. The copper deposition reaction occurred orders of magnitude slower than its light-limited rate. In addition to this, hot electrons will reduce copper(II)(*trans*-diene)$^{2+}$ to copper(I)(*trans*-diene)$^{+}$ at its light-limited rate in competition with the copper plating reaction. Thus, quantum efficiencies measured by this copper-plating reaction are much lower than the actual quantum efficiency for hot carriers being ejected into solution. This is the greatest limitation to our ability to measure hot carriers quantitatively using this system.

Quantum efficiencies for our experiments can be calculated by comparing the stripping current densities to the photon flux. Referring back to Table II, the maximum current density calculated from the photon flux for the high-doped electrode at 543.5 nm is $J_{calc}(max)$ = 250 μA/cm^2. The light-limited total current density was $J_{meas}(max)$ = 135 μA/cm^2, so the total current efficiency of the cell was 54%. Incomplete absorption of light in the depletion region as well as recombination in the bulk and at surface states limit the total current efficiency. The maximum stripping current density, $J_{strip}(max)$ for this experiment was 0.60 μA/cm^2. The stripping of copper is a one-electron process, so the measured hot photocurrent is equal to the stripping current. The measured quantum efficiency for copper plating by hot electrons is then $\phi_{Cu} = J_{strip}(max)/J_{calc}(max) \times 100 = 0.24\%$.

As previously discussed, the true quantum efficiency for hot electrons being ejected into the solution is undoubtedly higher than we have measured. Measurement of ϕ_{hot} is limited in our experiments by the fact that hot electrons are capable of reducing copper(II)(*trans*-diene)$^{2+}$ to copper(I)(*trans*-diene)$^{+}$ as well as reducing copper(I)(*trans*-diene)$^{+}$ to Cu(0) + *trans*-diene. The ratio of J_{strip} to J_{total} for the metal-like n-InP electrode at −1.6 V is 10^{-3}, which reveals that hot electrons being ejected into the solution at −1.6 V would be expected to reduce copper(I)(*trans*-diene)$^{+}$ to Cu(0) only 1/1000 of the time, assuming that the kinetics of the two processes are similar. This is why we have chosen to express the quantum efficiency in terms of copper-plating efficiency rather than a true hot-carrier quantum efficiency.

The only way a true hot-carrier quantum efficiency can be calculated is to use a probe molecule, which can be reduced at its light-limited rate by hot electrons with no competition from any other process. This is difficult to achieve because in order to avoid competition from other species, there must be no other reducible molecules present in the solution. We have found that the band-edge positions are sensitive to solution redox potential, so we must maintain a constant redox potential during the experiment. This requires that both the oxidized and the reduced forms of a redox couple be present.

On the basis of the base-line noise in the stripping voltammograms, we estimate that under the given experimental conditions the lowest stripping current density that can be determined is 0.05 μA/cm^2. This corresponds to ϕ_{Cu} = 0.02%, which is roughly 8% of the maximum ϕ_{Cu} of 0.25% that has been measured.

Doping Density Dependence. Hot photocurrent was observed only at high-doped p-InP. This was expected because of the wider

Table III. Depletion Region Calculations[a]

	doping density	applied potential, V			
		−0.5	−0.7	−0.9	−1.1
$V - V_{fb}$	high	0.600	0.800	1.000	1.200
	low	0.450	0.650	0.850	1.050
W_d, Å	high	228	263	294	322
	low	2280	2740	3130	3480
E_s, V/cm	high	2.63×10^5	3.04×10^5	3.40×10^5	3.73×10^5
	low	1.97×10^4	2.37×10^4	2.72×10^4	3.02×10^4
t_d, fs	high	1.88	1.88	1.88	1.88
	low	251	251	251	251

[a] Assumes: $V_{fb,high} = +0.1$ V and $DD_{high} = 1.6 \times 10^{18}$ cm^{-3}. $V_{fb,low} = -0.5$ V and $DD_{low} = 1.2 \times 10^{16}$ cm^{-3}.

space charge region and smaller electric field present at the surface of a low-doped electrode. Calculated values of the band bending ($V - V_{fb}$), the depletion region width (W_d), the electric field at the surface (E_s), and the time required for a photogenerated electron to traverse the width of the space charge region in the presence of that electric field (t_d) are presented for various applied potentials in Table III. These were calculated using the classical relations[3,29]

$$W_d = \left[\frac{2\epsilon\epsilon_0(V - V_{fb})}{qN_d}\right]^{1/2} \qquad E_s = \frac{V - V_{fb}}{W_d} \qquad t_d = \frac{W_d}{\mu E_s}$$

where N_d is the doping density, ϵ is the static dielectric, and μ is the electron mobility in the semiconductor. It is clear that, for equal amounts of band bending, the depletion region is approximately 10 times as wide and the electric field present is about a factor of 10 lower for the low-doped case. The result is that hot carriers are expected to be ca. 100 times more efficient for the high-doped electrodes than for the low doped. This doping density dependent behavior is further evidence that the copper plating seen on high-doped electrodes is the result of a hot-electron reduction.

Wavelength Dependence. In order to properly compare experiments of different wavelengths, we must compare quantum efficiencies rather than stripping current densities because the photon fluxes for the separate experiments were different. The maximum quantum efficiency for copper production by hot carriers (ϕ_{Cu}) calculated for the 543.5-nm experiment was 0.24%, while for 632.8 nm, it was 0.25%. Within the limits of experimental error, which we estimated to be 0.02%, there is no wavelength dependence observed. This is evidence for type I hot carriers, which is consistent with the observations of Nozik et al.[5] Type II hot carriers would be expected to yield much higher hot currents at shorter wavelengths because the hot electrons would be ejected with greater energies where the rate constant for copper deposition is much higher.

Intensity Profile Dependence. With the beam expanded so that the beam area was several times larger than the electrode area, greater stripping current densities were observed than when the area was smaller than the electrode surface. It is clear that the highly defocused laser is a much more uniform source than the slightly defocused laser since lasers exhibit Gaussian beam intensity profiles. The light intensity was more than 100 times larger in the center of the beam than at the edges of the electrode for the variable profile experiments, while it varied by only 5% for the uniform profile experiments. When an experiment is performed with the light beam smaller than the electrode, the center of the electrode is highly illuminated, while the edges are essentially in the dark.

In the variable-intensity profile experiments it is possible that local band-flattening effects served to decrease the band bending and thus decrease hot-carrier efficiencies. Also, when determining the band edges, the entire electrode surface contributes to the measured capacitance, so we cannot infer that the energetics of the electrode are the same in the center of the light beam as they are on the dark edge of the electrode. Overall, performing experiments with the laser area smaller than the electrode surface area does not appear to be a reliable way to obtain photoelectrochemical information.

Summary

1. Mott–Schottky analysis performed under the exact conditions of the plating experiment, along with voltammetric and plating experiments at n-InP in the accumulation condition, has established that the formation of copper at p-InP can only occur via a hot-electron reduction.

2. Copper produced by the supraband-edge reduction of copper(I)(*trans*-diene)$^+$ is believed to be the first observation of a chemical product produced by a hot-carrier reaction in a PEC.

3. Doping density dependence was both expected and observed. Copper plating was observed at high-doped electrodes but not at low-doped electrodes. The fact that no copper deposition occurs on low-doped p-InP supports the argument that copper deposition is a supraband-edge reaction.

4. Experiments done at 632.8 and 543.5 nm reveal there is no wavelength dependence, a result consistent with type I hot carriers being the dominant mechanism. This is in support of previous experiments done by Nozik et al.[5]

5. Measured quantum efficiencies for copper plating by hot electrons, (ϕ_{Cu}), reached a maximum of 0.24 and 0.25% for 632.8- and 543.5-nm experiments, respectively. The quantum efficiency for ejection of hot electrons into the solution is undoubtedly higher, since the copper(II)(*trans*-diene)$^{2+}$ + e$^-$ → copper(I)(*trans*-diene)$^+$ reaction occurs simultaneously.

6. When performing photoelectrochemical experiments with lasers, the light beam should be defocused to an area much larger than the electrode surface area to maintain a uniform-intensity profile across the entire electrode surface.

Acknowledgment. We thank Dr. John Turner of SERI for providing us with the capacitance software and for many useful discussions and Professor Nathan Lewis of the California Institute of Technology for suggesting the use of uniform-illumination profiles. This work was supported by the Department of Energy (Division of Chemical Sciences) under Contract No. DE-FG02-84ER13247. P.R.S. acknowledges the Link Foundation for a Link Energy Fellowship from Sept 1986 to Aug 1987.

(29) Wilson, R. H. Electron Transfer Processes at the Semiconductor-Electrolyte Interface. *CRC Critical Reviews in Solid State and Material Sciences*; CRC: Boca Raton, Fl, 1980; pp 1–4.